Strain Sensing in Thin Composite Laminates with Embedded Fiber Bragg Grating Sensors

BRAYDEN ALLER, SERGIO PELLEGRINO, NATHAN KINKAID, JUAN MEJIA-ARIZA, RICHARD OTIS, PATRICK HON MAN CHAN and FRANCISCO PENA

ABSTRACT

Ultra-thin fiber Bragg grating sensors were used to measure strain changes in thin composite laminates. The first part of the paper presents tension tests on thin composite laminates with embedded ultra-thin fiber Bragg grating sensors to measure the gage factor relating shifts in the fiber Bragg grating reflected wavelength to the laminate strains. The second part of the paper then investigates the ability of these embedded fiber Bragg grating sensors to accurately measure the internal strains of thin laminates in bending.

INTRODUCTION

Thin composite laminates are being increasingly used in the construction of deployable spacecraft structures. To ensure the reliability of these structures throughout their lifetime, it is of interest to be able to monitor their internal strain state and detect changes over time. Fiber optic sensors are particularly well suited for this task as they are lightweight and very flexible, enabling them to withstand the high curvatures required for the stowage of these structures. However, the problem with typical fiber optic strain sensors (125 μm cladding diameter) is that they are often too large for inclusion in thin composite laminates ($<$ 200 μm thick) without significant disruption to the laminate microstructure. To minimize the disruption of the embedded sensors on the thin laminates, it is crucial to have sensors with the smallest possible diameter. To this end, this work investigates the ability of ultra-thin (30 μm cladding diameter) fiber Bragg grating (FBG) sensors to accurately measure the internal strain state of thin composite laminates.

FBGs are a type of fiber optic sensor in which gratings with period Λ are inscribed within the optical fiber core. These gratings reflect a particular wavelength of light, λ, that is proportional to both Λ and the effective refractive index of the optical fiber, n, via:

$$\lambda = 2n\Lambda \tag{1}$$

Brayden Aller and Sergio Pellegrino, Graduate Aerospace Laboratories, California Institute of Technology, 1200 E California Blvd, MC 105-50 Pasadena, CA 91125, USA.
Nathan Kinkaid, Juan Mejia-Ariza and Richard Otis, Jet Propulsion Laboratory (JPL), California Institute of Technology, 4800 Oak Grove Dr, Pasadena, CA 91109, USA.
Patrick Hon Man Chan and Francisco Pena, NASA Armstrong Flight Research Center (AFRC), P.O. Box 273 Edwards, CA 93523, USA.

Changes in temperature or strain of the FBG cause shifts in λ that can be tracked over time and converted into temperature or strain measurements via the relationship:

$$\frac{\Delta\lambda}{\lambda_0} = \alpha\epsilon + \beta\Delta T \tag{2}$$

where $\Delta\lambda$ is the measured change in the reflected wavelength from the baseline value λ_0, α is the gage factor, ϵ is the FBG strain, β is the thermo-optic coefficient, and ΔT is the change in temperature from baseline. A number of works have demonstrated the ability of embedded FBG sensors to measure strains in composite laminates with some examples including the measurement of residual strain buildup during curing [1], the measurement of through-thickness strain distributions in bending [2], or the measurement of coiling strains [3].

However, little work has been done to investigate the use of these ultra-thin FBGs to measure strains in thin composite laminates, with the only previous work [4] demonstrating the successful embedment of these sensors in thin composite laminates and showing that the inclusion of these embedded sensors does not impact the bending stiffness or failure of similar thin laminates to those used in this work. The goal of this paper is to investigate the ability of these ultra-thin FBG sensors to accurately measure the internal strain state of thin composite laminates. This investigation is split into two parts. The first part measures the gage factor α of ultra-thin FBG sensors embedded in thin composite laminates through tensile testing. The second part then uses these measured gage factors to measure strains in these thin laminates as they undergo bending, which is of specific interest for the stowage of deployable composite structures. These measurements are then compared with an external estimate of strain at the FBG location to assess the accuracy of the internal FBG strain measurements.

MANUFACTURING OF THIN LAMINATES WITH EMBEDDED FBGS

For this work, two thin composite laminates with embedded ultra-thin FBG sensors were manufactured. These laminates were constructed out of 15 grams per square meter (gsm) unidirectional carbon fiber prepreg with MR70 carbon fibers and NTPT ThinPreg 402 epoxy resin with a layup of $[0_4/90_4/0_4]$. This resulted in laminates with a cured thickness of approximately 170 μm. Each laminate had one ultra-thin FBG sensor (30 μm cladding diameter) with a 10 mm gage length, procured from Redondo Optics, Inc., embedded in the outer 0° lamina parallel to the surrounding carbon fibers. The placement of the sensors here minimizes their intrusion into the thin laminates and enables them to measure bending strains by being offset from the laminate mid-surface. These laminates were each 60 mm in length and 20 mm wide with the embedded FBG located in the center. A cross-sectional image from a μCT scan of the FBG region of one of these thin laminates can be seen in Figure 1. The μCT scan was taken with a ZEISS XRadia 510 Versa 3D X-ray Microscope at a resolution of approximately 1 μm.

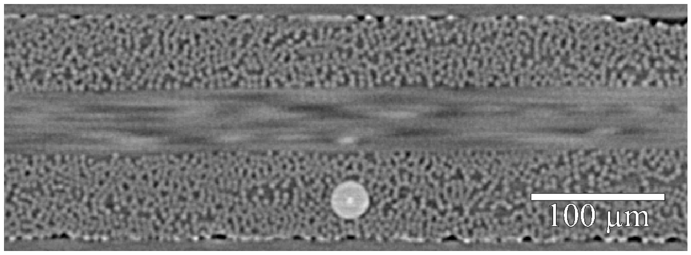

Figure 1. Cross-section of thin laminate with embedded FBG.

TENSILE TESTING OF THIN LAMINATES WITH EMBEDDED FBGS

Experimental Setup

The goal of this tensile testing was to measure the gage factor α of the embedded ultra-thin FBG sensors. To do this, the thin laminates with embedded FBGs were each mounted in wedge grips in an Instron load frame with the FBGs centered between the grips. A testing length of 30 mm between the grips was chosen so that the FBGs, which have a length of 10 mm, were sufficiently away from the clamped regions. These laminates were each subjected to small elastic tensile strains up to at least 250 $\mu\epsilon$ by slowly stretching them at a cross-head displacement rate of 0.1 mm/min. It was assumed that the tensile strains were uniform through the thickness of the laminates throughout testing and therefore that surface strain measurements could then be used to accurately measure the FBG strains. On the FBG-side of the laminates, a pair of 5-MP digital image correlation (DIC) cameras with 35 mm focal length lenses was used in conjunction with Correlated Solutions VIC-3D software to directly measure surface strains over the FBG regions during testing. On the opposite side of the laminates, a laser extensometer was used to provide a secondary external strain measurement of the FBG regions. The corresponding shifts in λ during tensile testing were measured with a Luna HYPERION si255 interrogator. All systems were time-synchronized for this testing and data was collected at a rate of 2 Hz. These tests were repeated five times for each laminate. The tension test setup can be seen in Figure 2.

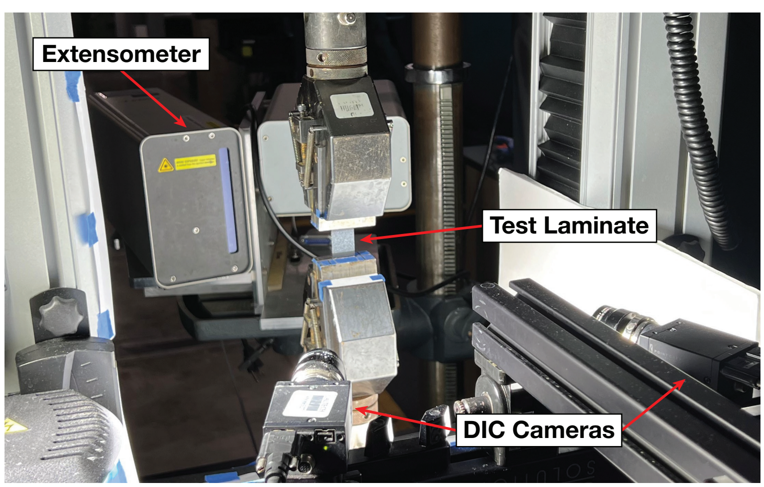

Figure 2. Tension test experimental setup.

Empirical Determination of α

To convert the experimental data into a measure of α, Eq. 2 can be rewritten as:

$$\frac{\Delta\lambda}{\lambda_0} = \alpha\epsilon \tag{3}$$

note the contribution of ΔT is neglected since this testing occurred in a temperature-controlled laboratory environment. Since there is a linear relationship between the experimentally measured $\Delta\lambda/\lambda_0$ from the embedded FBGs and the measured strain ϵ, linear regression was used to find the value of α that provides the best fit between the two data sets.

The strain data used in these regression analyses was taken from the DIC data by finding the average strain in a 10 mm long $\times$ 2 mm wide box over the FBG region at every time step. This was done since the measurement output by each FBG is an average over its gage length of 10 mm. It is noted that the additional strain data collected from the laser extensometer was not used in these analyses since the quality of this data was poor, in part due to the short testing length over which it was measuring. The strain data was then plotted against the corresponding $\Delta\lambda/\lambda_0$ data and linear regression analyses were performed for all five trials for each of the laminates. An example plot can be seen in Figure 3.

The mean and standard deviation of α over all five trials for each laminate are presented in Table I. It is noted that all analyses for α had an $R^2 > 0.9$ with all but two being > 0.94 indicating good linear fits for all of the data sets.

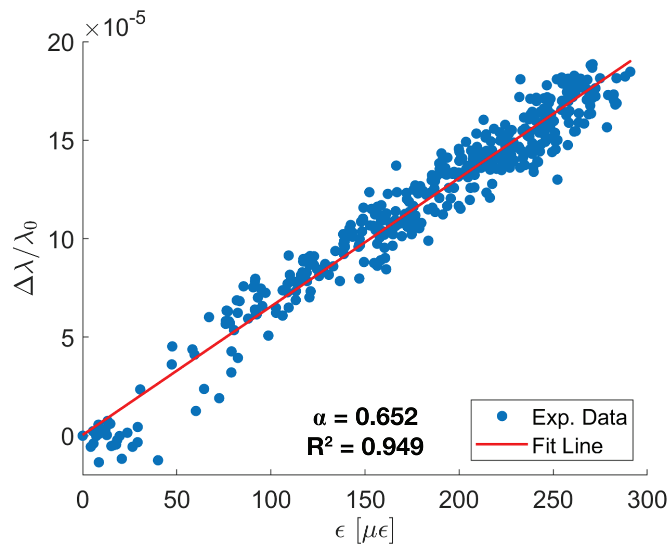

Figure 3. Experimental results from Laminate 1 Test 3.

TABLE I. α EXPERIMENTAL RESULTS

	Mean	STD
Laminate 1	0.664	0.021
Laminate 2	0.634	0.026

In Table I it can be seen that the mean values of α for both laminates were close together, but with a slight difference between them. As seen in the standard deviations for each α, there were some variations in these values between different trials. To further investigate these issues and get better measures of α, this testing will be repeated in the future for greater strain ranges and with a larger number of trials for each laminate. It is noted that both of these values of α are less than the typical value for FBGs, which is around 0.78 [5]. The cause for this difference will be explored in future work.

STRAIN MEASUREMENTS OF THIN LAMINATES IN BENDING

Experimental Setup

Bending is a common loading condition that thin composite laminates face in their lifetime. It is therefore important to assess the ability of these embedded ultra-thin FBG sensors to accurately measure the bending strains of thin composite laminates. To do this, the same two thin laminates with the embedded ultra-thin FBG sensors were bent using the column bending test (CBT) fixture mounted in an Instron load frame.

The laminates were each mounted in the CBT fixture with a free length, or length between the rigid arms of the fixture, of 20 mm with their FBG located in the center. This was chosen to ensure that the FBGs were within the region to be bent and were sufficiently away from the clamped regions to avoid edge effects. These coupons were each bent at a cross-head displacement rate of 5 mm/min for two minutes yielding a maximum imposed curvature of approximately 40.5 m^{-1}, which is well away from the failure curvatures measured in similar laminates in [4]. These samples were each held at this curvature for ten seconds and then returned to the flat state at 5 mm/min. This test was repeated six times for each laminate, with three of these trials occurring when the FBGs were on the tension side of the laminates in bending, and three when they were on the compression side. On both sides of the load frame, a pair of 5-MP DIC cameras with 35 mm focal length lenses was used to directly measure the surface strains of these laminates as they underwent bending. This strain data was then processed using VIC-3D software from Correlated Solutions.

The FBG measurements were taken with the Luna HYPERION si255 interrogator and the wavelength measurements were converted into strains using the empirically measured mean values of α for each laminate found in Table I. Both FBG and DIC measurements were taken at a rate of 2 Hz throughout the tests and all systems were time-synchronized. This experimental setup can be seen in Figure 4.

Secondary Estimate of FBG Strain Measurements

To assess the accuracy of the internal FBG strain measurements, estimates of strain at the FBG locations within the laminates were needed. Doing this required surface strain measurements from the regions over the embedded FBGs and accurate measurements of laminate thickness and position of the FBGs relative to the mid-surface of the laminates. The surface strains were directly measured on both sides of the laminates using the two synchronized DIC systems. The surface strain measurements over the embedded FBGs were obtained by taking the average strains from the DIC strain data in 10 mm long

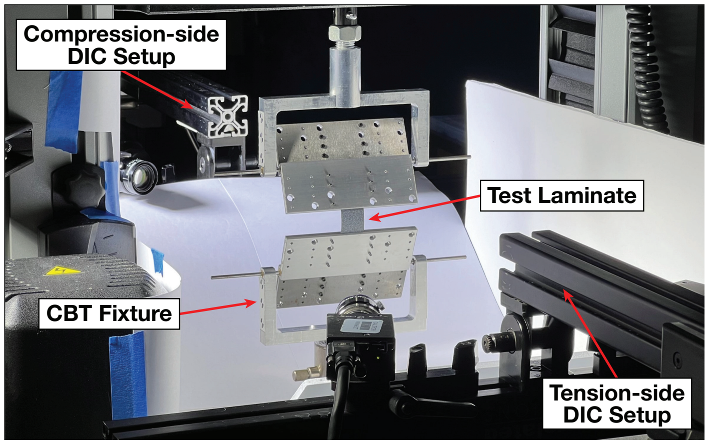

Figure 4. Bending experimental setup.

$\times$ 2 mm wide boxes centered over the FBGs on both sides of the laminates. To get accurate measurements of laminate thickness and embedded FBG position, μCT scans of both laminates were taken with a ZEISS XRadia 510 Versa 3D X-ray Microscope at a resolution of 1 μm. To account for variations in FBG position and laminate thickness along their length, approximately 6 mm long scans were taken in the center of each FBG region. This accounts for more than half of the length of these sensors and is therefore assumed to provide a good approximation of these variations over the full length of the FBGs. Within each of these scans, 61 measurements of both FBG position and thickness were taken in approximately uniform increments along the scan length. These were then averaged to get a good representation of them throughout the FBG length. Since the DIC surface strain measurements were obtained by tracking speckles in a thin layer of paint added to the surface of the laminates before testing, the thickness of this paint was included in the laminate thickness and FBG position measurements.

Once this data was processed, estimates of strain at the FBG location in each laminate were generated. By assuming a linear strain variation through the laminate thickness in bending, the surface strain measurements and laminate thickness measurements enabled the calculation of the strain gradient through each laminate at every time-step. The average FBG position measurements were then used to determine their location in their strain gradient and generate an estimate of the strain they each experienced at every time-step.

Comparison of Strain Measurements

To provide a comparison between the strains measured by the FBG and the strain estimate, the difference between the two curves as they were held the highest strain state was found. This was done by calculating the percent difference between average strains each measure of strain reported during this time. The results of these comparisons are presented in Table II for the compressive strain case and Table III for the tensile strain case. Examples plots comparing FBG and estimated strain curves are presented in Figures 5(a) and 5(b) for a compressive strain test and tensile strain test respectively.

In general, there was good agreement between the FBG and strain estimates with most of the tests falling within 6.5% of each other with the exception being the Laminate

TABLE II. FBG COMPRESSIVE STRAIN COMPARISON [% DIFFERENCE]

	Test 1	Test 2	Test 3
Laminate 1	-0.64	1.59	-0.37
Laminate 2	6.11	6.09	5.65

TABLE III. FBG TENSILE STRAIN COMPARISON [% DIFFERENCE]

	Test 1	Test 2	Test 3
Laminate 1	5.22	4.71	5.38
Laminate 2	17.33	16.84	15.98

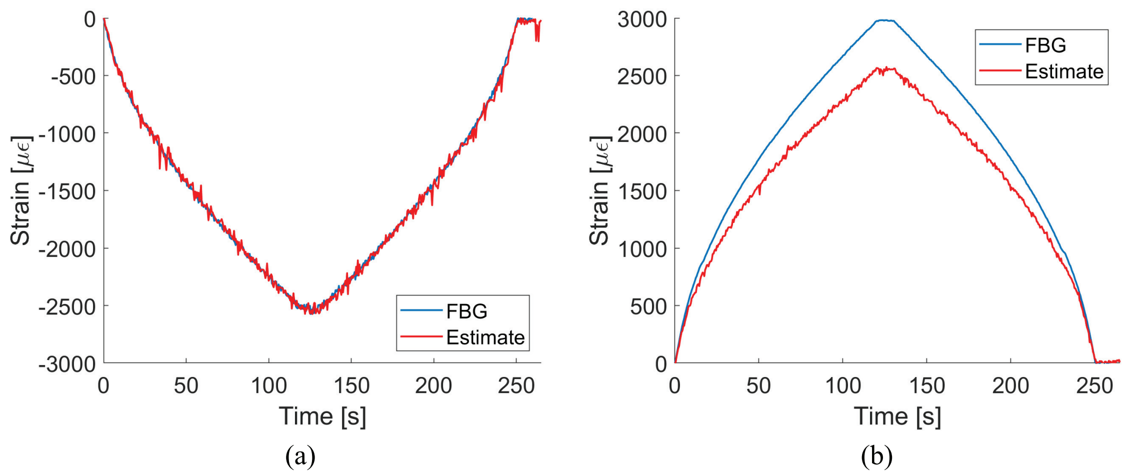

Figure 5. (a) Comparison of FBG and estimated compressive strain data for Laminate 1: Test 3 and (b) comparison of FBG and estimated tensile strain data for Laminate 2: Test 2.

2 tension-side tests falling within 17.5%. In Figures 5(a) and 5(b), it can be seen that regardless of the differences in strains between the curves, the FBG strain measurement curve always follows the same general profile as the estimated strain curve: increasing in amplitude for the first 120 seconds, plateauing for 10 seconds as the laminate is held, and then decreasing back to zero strain in the last 120 seconds. This indicates that the embedded FBGs measure the internal change in laminate strain as a result of bending, but that errors in either our gage factors or strain estimates are leading to inaccuracies in one or both of these measurements. This indicates that further work to remove these errors is needed to fully validate the accuracy of these sensors in measuring the strain state of these thin composite laminates. A discussion of some possible errors follows.

In the context of the strain estimates at the FBG locations, there are two possible sources of error.

The first relates to errors in the laminate thickness and FBG position measurements. While over half of each FBG region was scanned, it is possible that there are variations in laminate thickness and FBG position outside of the scanned regions that go unaccounted for in the strain estimates, but influence the strain the FBGs measure in bending. In a similar vein, the contribution of the DIC paint to both the total thickness and FBG position measurements may lead to errors. While the paint is assumed to not significantly affect the bending behavior of the laminate since it is a thin layer and has a small modulus relative to the laminate, it may contribute to errors in the strain estimates due to its high thickness variability. It was observed that the paint varies in thickness from a few μm thick in some places to 10+ μm thick in others, which could skew thickness and FBG position measurements in the laminate. A further investigation into the influence of paint on the strain estimates will be conducted in future work.

The second possible source of error is a small error in the FBG location between the CBT grips. While confidence in its position is high due to careful measurements and laminate placement, it is possible that the FBG was slightly shifted away from its desired location in the center of the CBT fixture. This would then make the strain data extracted from the DIC systems inaccurate for the actual FBG location and could lead to errors in the strain estimate.

CONCLUDING REMARKS

In this work, measurements of the gage factor of ultra-thin FBG sensors embedded in thin composite laminates were successfully obtained through tensile testing. Additionally, the ability of embedded ultra-thin FBG sensors to measure strains in thin composite laminates under bending was proven. However, the accuracy of the amplitude of the measured strains was not fully validated and further work will be conducted to both refine the gage factor measurements, and investigate possible sources of error preventing the full validation of these internal strain measurements.

ACKNOWLEDGMENTS

The research was carried out in part at the Jet Propulsion Laboratory, California Institute of Technology, under a contract with the National Aeronautics and Space Administration (80NM0018D0004). Support from the Caltech Space Solar Power Project is acknowledged.

REFERENCES

1. Takagaki, K., S. Minakuchi, and N. Takeda. 2017. "Process-induced strain and distortion in curved composites. Part I: Development of fiber-optic strain monitoring technique and analytical methods," *Composites Part A*, 103:236–251.
2. Bosia, F., M. Facchini, J. Botsis, T. Gmür, and D. de'Sena. 2004. "Through-the-thickness distribution of strains in laminated composite plates subjected to bending," *Composites Science and Technology*, 64(1):71–82.
3. Aller, B., S. Pellegrino, N. Kinkaid, J. Mejia-Ariza, R. Otis, P. Chan, and F. Pena. 2022. "Health Monitoring of High Strain Composites Using Embedded Fiber Bragg Grating Sensors," in *AIAA SciTech 2022 Forum*, p. 1622.
4. Aller, B., S. Pellegrino, N. Kinkaid, J. Mejia-Ariza, R. Otis, P. Chan, and F. Pena. 2023. "Strain Measurement in Coilable Thin Composite Shells with Embedded Fiber Bragg Grating Sensors," in *AIAA SciTech 2023 Forum*, p. 2399.
5. Kashyap, R. 2010. *Fiber Bragg Gratings*, Academic Press, 2nd edn.